Received: 15 June 2022 | Revised: 25 September 2022 | Accepted: 6 October 2022

DOI: 10.1002/jemt.24247

RESEARCH ARTICLE

MICROSCOPY RESEARCH & TECHNIQUE WILEY

Identification of *Hypoderma actaeon* (Diptera: Oestridae) in red deer (*Cervus elaphus*) from northern Spain: Microscopy study and molecular analysis

Sara González[1] | Maria Luisa Del Rio[2] | Maria Natividad Diez[1] | Maria del Rosario Hidalgo[1] | Angelica Martínez[3]

[1]Department of Animal Health, Parasitology and Parasitic Diseases, Faculty of Veterinary Science, University of León, León, Spain

[2]Department of Animal Health, Section of Immunobiology, Faculty of Veterinary Science, University of León, León, Spain

[3]Department of Biotechnology and Food Science, Faculty of Sciences, University of Burgos, Burgos, Spain

Correspondence
Maria del Rosario Hidalgo, Parasitology and Parasitic Diseases, Department of Animal Health, Faculty of Veterinary Science, University of León, 24071 León, Spain.
Email: mrhida@unileon.es

Funding information
"Ministerio de Ciencia y Tecnología, Grant/Award Number: FIS PI16/00002; Ministerio de Ciencia y Tecnología, Grant/Award Number: 2004-02580-C03-03/BOS; European Union

Review Editor: Alberto Diaspro

Abstract

Hypoderma spp. larvae were observed subcutaneously in the dorsal and lumbar regions of red deer (*Cervus elaphus*) hunted in the province of León (northwestern Spain) causing a myiasis. They were removed and initially classified by their size, shape, color, and location under the skin into the three larval stages that parasitize these animals. The morphological characteristics of the first and second-instar are described and from the features of the third-instar the species was identified as *Hypoderma actaeon*. To accurately identify this species, five isolates of genomic DNA from the third-instar, two from the second-instar and two from first-instar of *H. actaeon* were analyzed by PCR analysis of the COI region of mt-DNA. The results confirmed that the examined samples exactly matched with *H. actaeon*. This study has shown the morphological identification of the three larval stages of *H. actaeon* and, for the first time, the first and second-instar larvae have been molecularly characterized. Finally, identification of only *H. actaeon* suggests that this species is the only affecting red deer in the Iberian Peninsula.

KEYWORDS
hypodermosis, light microscopy, molecular analysis, morphology, red deer, SEM, Spain

Research Highlights

- Description, for the first time, of first and second-instar *Hypoderma actaeon* through light microscope and stereomicroscope.
- Morphological Identification of third-instar *H. actaeon* by SEM observations.
- Molecular characterization of *H. actaeon*.

1 | INTRODUCTION

Hypodermosis is a subcutaneous myiasis caused by the genus *Hypoderma* (Diptera, Oestridae) whose species have an annual life cycle, affect domestic and wild animals of the Bovidae and Cervidae families and are distributed in the Holarctic ecozone (Zumpt, 1965).

The most common and most studied species are *Hypoderma bovis* and *Hypoderma lineatum*, which mainly affect cattle (*Bos taurus*).

Hypoderma actaeon is a typical parasite of red deer (*Cervus elaphus*) and is considered strictly host-specific (Brauer, 1863). It is the species found in *C. elaphus hispanicus* in the Iberian Peninsula and its presence has been reported in several regions of Spain (De la Fuente-López et al., 2001; Domínguez et al., 2010; Gil-Collado et al., 1984; Hernández et al., 1980; Martínez-Gómez et al., 1990; Martínez-Moreno et al., 1997; Panadero et al., 2010; Pérez et al., 1995; San Miguel et al., 2001) and Portugal (Ahmed et al., 2017). Despite its specificity this parasite has been occasionally reported in cattle, fallow deer and roe der (Ahmed et al., 2017; Panadero et al., 2010, 2017).

During a study in a hunting reserve from northern Spain with coexisting wild and domestic ungulates we had the opportunity of examining a large number of red deer with different larval stages of *Hypoderma*. The purpose of the present research was to identify larval stages of *H. actaeon* based on their morphology and molecular analysis.

2 | MATERIALS AND METHODS

2.1 | Study area and sampling procedures

The present study was undertaken in the Riaño Regional Hunting Reserve (43°03′14″ N, 4°57′33,85″ W), Province of León, northwestern Spain and located in the Cantabrian Mountains. A total of 110 red deer were studied, most of them were shot by the technical staff of the reserve in selective hunting. The inner surface of the skin was carefully examined to check the existence of alterations such as bleeding, congestion, abscesses, cysts or nodules. Subcutaneous larvae of *Hypoderma* spp., in all three stages (Figure 1a), were found in the dorsal and lumbar regions of the animals and their anatomical position was noted. They were removed and initially classified by their size, shape, color, and location under a thin layer of fibrous connective tissue or inside subcutaneous nodules with their breathing hole to the outside. Later they were counted, measured and preserved at −20°C and in 70% ethanol until the further study.

2.2 | Morphological identification of *Hypoderma* spp.: microscopy study

The morphological identification of *Hypoderma* was carried out mainly on third-instar larvae because they are the most studied and in which the most descriptive and distinguishable characteristics are indicated according to Colwell et al. (1998) and Otranto, Colwell, et al. (2003). For this, we use the scanning electron microscope observations. The third-instars were separated into three portions using the posterior three segments and the anterior four segments for their study. Samples were fixed with 2.5% glutaraldehyde, post-fixed with 2% osmium tetroxide, rinsed with PBS and dehydrated in aqueous ethanol at increasing concentrations for 30 min each step (30%, 50%, 70%, 90%, 3 × 96%, and 3 × 100%). Afterwards, the samples were dried using the critical point method using carbon dioxide as a transitional fluid for the total elimination of the dehydrating liquid. Immediately afterwards, the samples were mounted on cylindrical metal supports, coated with a conductive silver glue and then metalized with gold. The samples thus prepared can be observed under the SEM (JSM-6480 LV, JEOL, Tokyo, Japan) obtaining digital images at different magnifications.

At the same time, the two previous larval stages were placed between two trichinoscopy plates to flatten them and then they were

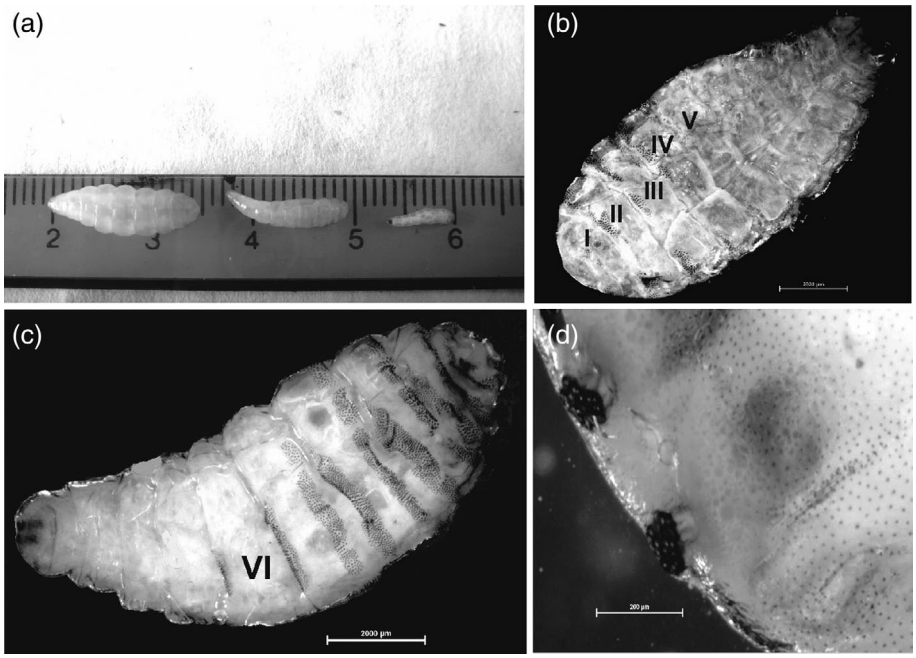

FIGURE 1 Larval stages of *Hypoderma actaeon*. (a) Initial classification. (b) First-instar *Hypoderma actaeon*. Dorsal view. Note the presence of small groups of spines only in the anterior margin of the first five thoracic segments. (c) Ventral view. Note the arrangement of the spines, much more numerous, on the anterior and posterior margins of the first five thoracic segments. In the sixth segment, only a small group of spines are seen on both margins and the rest of the segments lack them. (d) View of the respiratory openings in the posterior abdominal segment. Each spiracular plate has 16–18 spiracular openings. Note that this segment is all covered with small denticules

mounted on a slide in temporary preparations with 0.05% lactophenol cotton blue stain that allows the lightening and coloration of certain structures or in semi-permanent preparations with glycerinated gelatin that allows the mounting of unstained specimens neither dehydrate or in permanent preparations with a resin or synthetic resins after dehydration in successive baths of alcohols of increasing gradation. Thus, we were able to observe the peritreme features and the spination on larval segments, according to Zumpt (1965) and Sugar (1976), using stereomicroscope (Nikon SMZ 1500, Tokyo, Japan) and light microscope (Nikon YS-CF 100, Tokyo, Japan).

2.3 | Molecular analysis

The differentiation of *H. actaeon* was done on the mitochondrial gene enconding for the subunit 1 of cytochrome c oxidase (COI) and its subsequent amplification by PCR (Otranto, Colwell, et al., 2003).

2.3.1 | DNA extraction

The internal tissues of five third-instar, two second-instar and two first-instar *H. actaeon* were digested according to Green and Sambrook (2012). DNA samples obtained were quantified using a Nanodrop spectrophotometer (Thermofisher) and 50 ng of each sample were used for PCR amplification.

2.3.2 | PCR amplification and purification of PCR products

COI gene was amplified using the pair of primers UEA7 (5′-ACAGTTGGAATAGACGTTGATAC-3′) and UEA10 (5′-TCCAATGCACTAATCTGCCATATTA-3′), previously described by Otranto, Colwell, et al. (2003). The expected size of the PCR products was 688 base pairs. PCR products were subsequently analyzed using the GeneJET Gel Extraction Kit (Thermofisher), following the manufacturer's indications.

2.3.3 | Sequencing analysis and comparison of the sequences

Purified PCR products were sequenced using Thermosequenase cycle sequencing kit in the sequencing DNA core facility of the University of León. Reference sequences obtained from Genbank corresponding to *H. bovis* (KT600293), *H. actaeon* (AF497765), and *H. lineatum* (KP965726) were compared and aligned with the nucleotide sequences obtained from our amplified samples belonging to the third-instar using Clustal W (McWilliam et al., 2013). The sequences obtained from second and first-instar were compared only with that of *H. actaeon* (AF497765).

3 | RESULTS

3.1 | Morphological identification

3.1.1 | Light microscopy and stereomicroscopy

First-instar

They were found encapsulated in connective tissue under the skin of the dorsal and lumbar regions of the animals without observing any subcutaneous nodule or breathing hole to the outside. They are small, cylindrical slightly longer than wider and narrower ends, whitish or grayish, 5–10 mm long and 2–4 mm wide ($\bar{x} = 7.4 \pm 1.2 \times 2.5 \pm 0.7$ mm; $n = 20$).

They present bands of spines on their dorsal and ventral sides. These are small with broad bases and pointed tips.

The dorsal surface is less spiny than the ventral, with small groups of spines mainly on the anterior margin, extending to the third or fourth segment and the rest of the segments being bare (Figure 1b). They present a cephalic and caudal orientation indistinctly. Ventrally, the cephalic segment presents a group of spines at the level of the mouth opening. The mouth hooks are not externally visible and the cephaloskeleton is apparently weak. The thoracic segments have a double row of spines. Those of the anterior margin extend along its entire width and are caudally orientated while that of the posterior margin extends only to a little more than half and are cephalic directed. This pattern repeats until the fifth segment. In the sixth segment, in the center or laterally, sometimes only a group of spines oriented cephalically is observed, after which the segments are naked (Figure 1c). The last abdominal segment is covered with small denticles. In it, the spiracular plates often appear as two tubes with a circular opening. In a more advanced stage of its development it is observed that each spiracular plate is quadrangular or irregular in shape and is composed of 16–18 spiracular openings surrounded by a raised cuticular rima but we have not appreciated any spine on it (Figure 1d). It has not been possible to obtain images of these larvae with the SEM.

Second-instar

This larval stage was found inside the warble observing the breathing hole. It is elongated and thin, rounded at the anterior end and the posterior sharper, 10–17 mm long and 3–5 mm wide ($\bar{x} = 15.3 \pm 1.4 \times 3.6 \pm 0.6$ mm; $n = 20$) and yellowish to light brown in color. It has bands of spines on the dorsal and ventral side of the larva. These have the same shape as those of the first-instar with the same orientation but in greater number giving place to wider bands.

In the cephalic segment the mouth hooks are strong. Only one row of spines and not complete, it is observed dorsally in the anterior margin of the first three segments. Occasionally small groups of spines, with cephalic orientation, are located on the posterior margin of the second and third segment. In the fourth and fifth only small groups of spines are observed and the rest of the segments devoid of them (Figure 2a).

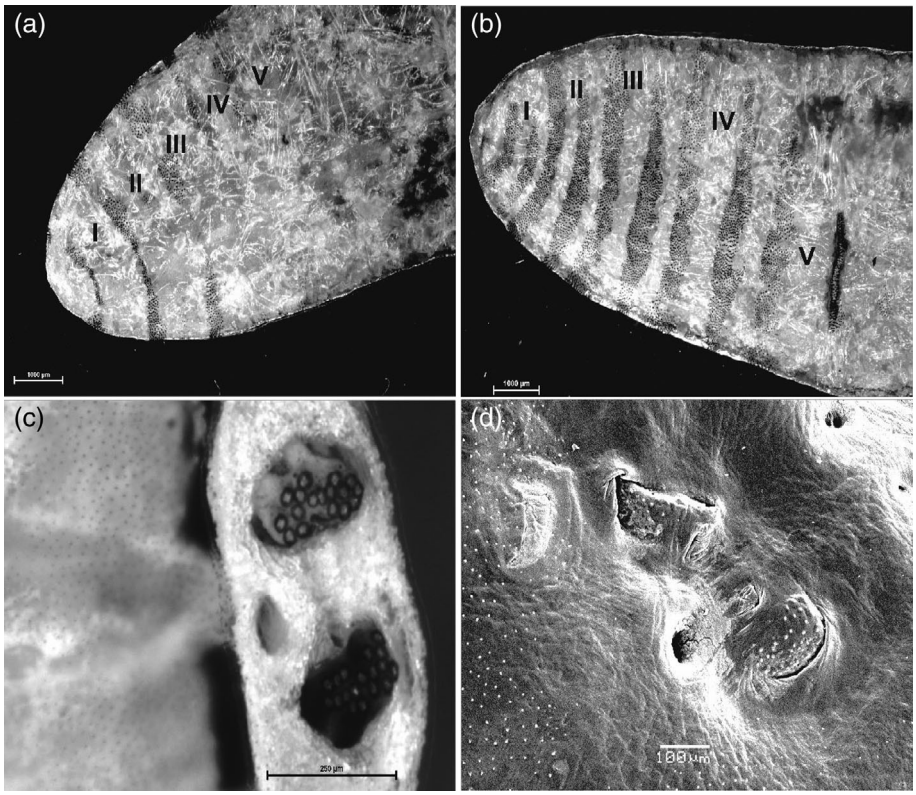

FIGURE 2 Second-instar of *Hypoderma actaeon*. (a) Dorsal view. Note an incomplete row of spines in the first three thoracic segments and only small groups in the fourth and fifth segment. The rest of segments are devoid of spines. (b) Ventral view. Note the presence of two bands of spines and its orientation in the anterior and posterior margins of the first five thoracic segments. (c) View of posterior spiracles. Spiracular plates with 18 openings, a single ecdysal scar on one side of one of the plates, and the anus located medially. (d) The spiracular plates are rising and initiating the characteristic C-shape. Observe the presence of small denticules in this last segment

Ventrally, the cephalic segment presents a group of spines below the mouth. In the thoracic segments, there are a greater number of spines arranged in two wider bands on the anterior and posterior margins of each segment. Those from of the first to the fifth thoracic segments are incomplete and in the sixth there is only a small group in each margin. The rest of the segments are not providing of spines (Figure 2b).

In the last abdominal segment, the spiracular plates have between 16 and 20 openings, observing the ecdysal scar on one side and the anus above (Figure 2c). In its last stage of development and already molting to three-instar, the electron microscope showed the rounded spiracular plates, rising and with a spine in each cuticular rima to later develops the characteristic raised C shape with many more spiracular openings and the ecdysal scar on one side (Figure 2d). As in first-instar, this last abdominal segment is covered of small denticles. It was also not possible to obtain good images of these larvae at SEM.

3.1.2 | Scanning electron microscopy

Third-instar

They were also found inside the warble with the peritreme in the breathing hole open in the skin. They are large and cylindrical, reaching 15–25 mm in length and 6–14 mm in width ($\bar{x} = 20 \pm 3 \times 11 \pm 2.3$ mm; $n = 20$) and ranged in color from yellowish to completely black. The cuticle has a granular appearance.

The cephalic segment is characterized by the absence of a band of spines between the oral opening and the opercular scar and the presence of a small band of spines ventral to the mouth with board bases, sharped tips and caudally directed (Figure 3a). The mouth hooks are strong, well developed and oriented at an angle to the anterior–posterior plane of the body with the smooth outer surface (Figure 3b,c).

The thoracic segments, on their ventral side, have a double row of spines. In the first, in apical view, four small groups of spines are arranged on both sides of the segment. Dorsal and ventrally there is a large group of spines that appear to be formed by the union of two small groups similar to the lateral ones (Figure 3a). All groups of spines are associated with cuticular sensilla located below each one of them or laterally (Figure 3b). The spines, although larger in size, have the same shape as those located below the mouth and are also caudally directed. In the lower part of the segment there is a row of spines with narrow bases, sharp tips and cephalic orientation. This pattern is repeated in the following thoracic segments. In the eighth segment, only a row of spines is observed in the anterior margin and the ninth and tenth segments lack spines both dorsally and ventrally.

In the last abdominal segment, the spiracular plates are shaped like a "C" and its inverse, with the ecdysal scar in the center, completely surrounded by the plate and deeply sunken in it. Around it, foliaceous elements are observed. The spiracular plates have numerous openings each surrounded by a raised cuticular rima and ornamented with a spine. As in the previous larval stages this segment is covered with small denticles. The anus is located between the spiracular plates (Figure 3d).

One larva was found encapsulated in fibrous connective tissue, covered only by a thin layer, without forming a subcutaneous nodule

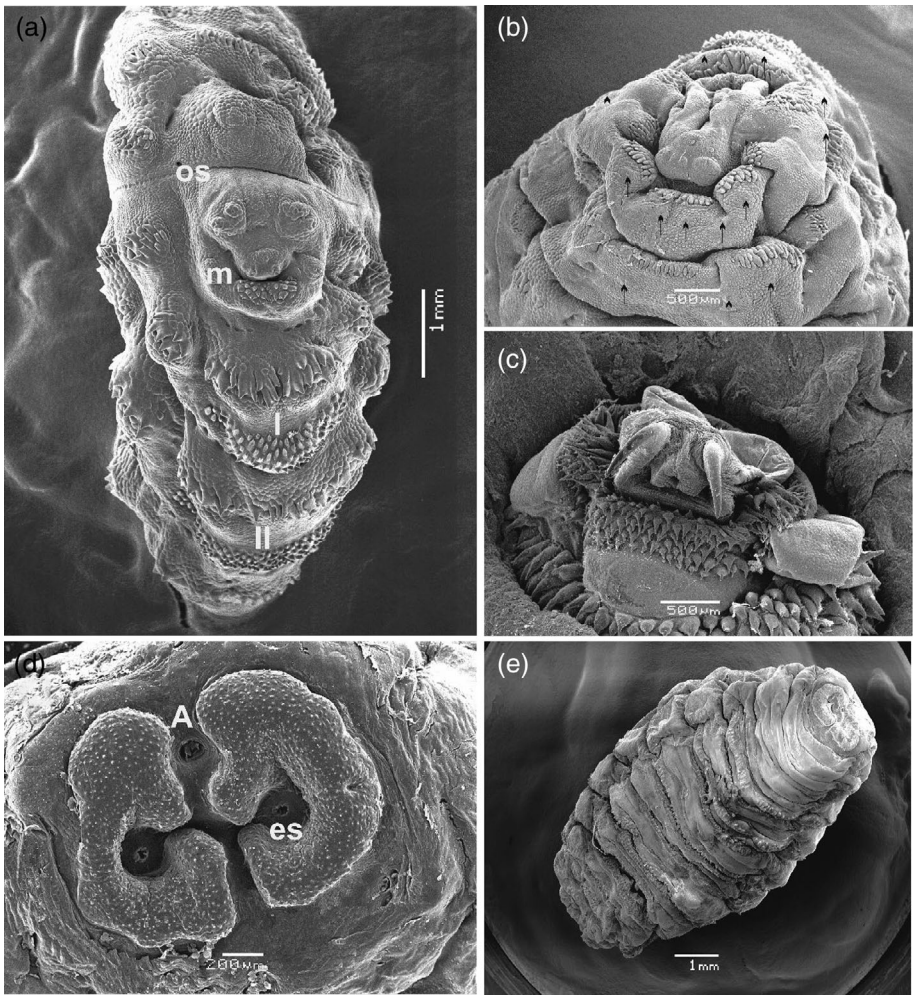

FIGURE 3 Third-instar *Hypoderma actaeon*. (a) Apical view of the cephalic and first two thoracic segments. In the cephalic segment observe the absence of a band of spines between the mouth (m) and the opercular scar (os). In the I and II thoracic segments note the arrangement of the spines. (b) Apical view of the cephalic segment showing the beginnings of the evagination of mouth hooks. Arrows show cuticular sensilla located below each spine cluster on the first and second thoracic segment. (c) Note the well-developed mouth hooks and antennal lobes in the cephalic segment. (d) Note the paired posterior spiracular plates with the ecdysal scar in the center and completely surrounded by the spiracular plate. On its surface, a small spine is associated with the rima of each spiracular opening (es: ecdysal scar; a: anus). (e) Ventral view of third-instar *Hypoderma actaeon*. This larva was found encapsulated in fibrous connective tissue. It did not form any warble and no breathing hole was observed to the outside. For this reason and also because of its small size it was classified as L1 until it was studied later. Note in ventral view, the arrangement of the spines in the segments, their absence in the ninth and tenth segments, and the characteristic fully developed spiracular plates

or breathing hole to the outside and classified as first-instar larvae, also due to its small size, color and weak aspect. After its study it was shown it was a fully developed third-instar larvae as can be seen in the Figure 3e.

3.2 | Molecular analysis

Five genomic DNA isolates from third-instar *Hypoderma* (V5, V7, V47, V54, and V107) were examined by PCR analysis of the COI region of mt-DNA. PCR amplification produced a nucleotide sequence of 666 base pairs. Blast analysis of the mitochondrial COI sequences was performed, taking from GenBank the sequence of *H. actaeon* AF497765 as reference and comparing it with those obtained by us. It was confirmed that the five-isolates samples exactly matched *H. actaeon*.

The sequences were deposited in Genbank with the following accession numbers: *H. actaeon* V5 (MZ696571), *H. actaeon* V7 (MZ700686), *H. actaeon* V47 (MZ700687), *H. actaeon* V54 (MZ700688), and *H. actaeon* V107 (MZ700689).

Then, the sequences were compared with reference sequences from *H. bovis* (KT600293), *H. actaeon* (AF497765), and *H. lineatum* (KP965726). Results from the alignments confirmed that the five samples matched with that of *H. actaeon* with a degree of interspecific difference of 0.291%. The degree of interspecific difference between the five samples and the reference sequences from *H. bovis* and *H. lineatum* was 12.35% and 12.06%, respectively (Figure 4).

We also collected samples from first- and second-instar larvae and blast analysis of mitochondrial COI sequences evidenced that the isolates corresponded with *H. actaeon* (Figure 5) with a degree of interspecific difference of 0.3%. The sequences are also available in Genbank with the following accession numbers: *H. actaeon* V82-L1 (ON540296), *H. actaeon* V90-L1 (ON540297), *H. actaeon* V31-L2 (ON540298), and *H. actaeon* V34-L2 (ON540295).

4 | DISCUSSION

The description of *H. actaeon* larvae is scarce and is mainly based on the morphology of the third-instar larvae. In this study, its identification was based on the characteristics mentioned by Colwell et al. (1998) and Otranto, Colwell, et al. (2003). In addition to these characteristics, we must point out the presence of small denticles in the last

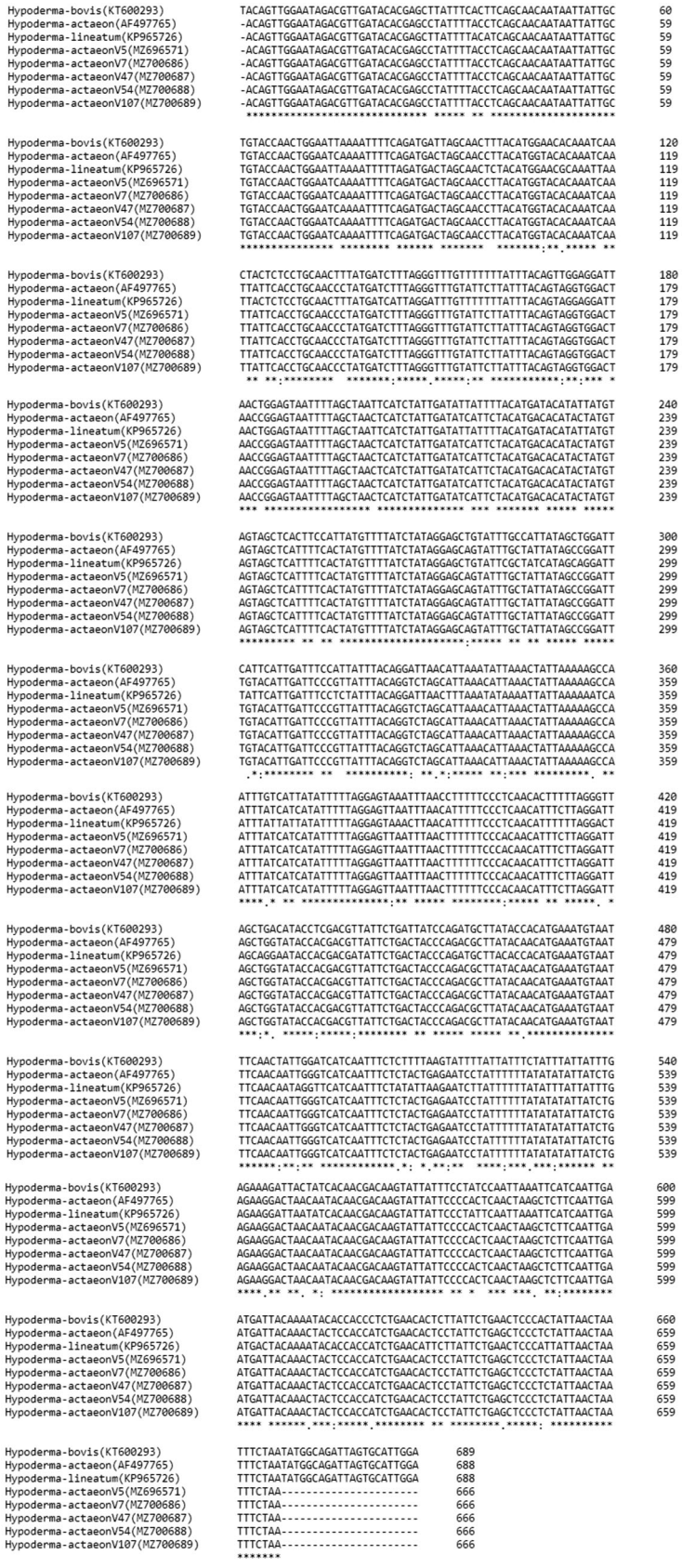

FIGURE 4 Alignments of the COI sequences from five field isolates compared with the reference sequences from *Hypoderma actaeon* (AF497765), *Hypoderma bovis* (KT600293), and *Hypoderma lineatum* (KP965726). Identical bases indicated perfect alignment and are shown by an asterisk (*). A site belonging to group exhibiting strong similarity or weak similarity are represented by (:) or (.), respectively

abdominal segment and in the three larval stages, a feature that no author has mentioned in this species and that Brauer (1863) only mentioned in the second-instar *Hypoderma* larvae.

Studies based on the external morphology of second-instar are limited and, in many cases, confusing and erroneous. Thus, Zumpt (1965) pointed out that its morphology was similar to that of *H. diana*,

FIGURE 5 Alignments of the COI sequences from first- and second-instar larvae field isolates compared with the reference sequences from *Hypoderma actaeon* (AF497765). Identical bases indicated perfect alignment and are shown by an asterisk (*)

with the same spination pattern on the dorsal and ventral side of the larva, which differs considerably from what was observed in this study.

In the reviewed bibliography we have not found any description of the morphology of *H. actaeon* first-instar, only some notes about its size, shape and color but referring in general to the genus *Hypoderma* (Colwell, 2001, 2006; Teskey, 1981).

We must point out that only San Miguel et al. (2001) shows some images of the three larval stages of this species in deer but does not describe them and Panadero et al. (2017) cites their finding in roe deer, giving only their localization under the skin and its size.

Thus, the lack of previous studies with accurate descriptions of the first- and second-instar larvae from this species precludes the comparison with our results.

By its part morphological identification of third-stage *Hypoderma* larvae can sometimes be difficult due to inadequate preservation of the larvae with remains of connective tissues, detritus or bacteria on its surface and their dark color, which is sometimes complicated to observe the spination pattern of the segments and the characteristics of the spiracular plates. Moreover, the possibility of the recovered larvae belonging to different *Hypoderma* sp. cannot be ruled out since red deer coexist with other wild and domestic ungulates. Thus, a more reliable method to identify *Hypoderma* larvae such as the molecular characterization is required.

The mitochondrial gene COI has been revealed to be an important molecular marker that allows the identification of the different species of flies that parasitize domestic and wild animals causing myiasis including those belonging to the families Oestridae (Ahmed et al., 2017; Otranto, Colwell, et al., 2003; Otranto, Traversa, et al., 2003), Calliphoridae (Wells & Sperling, 2001) and Sarcophagidae (Wells et al., 2001).

Results from the alignments confirmed that all the isolated samples matched with *H. actaeon* with a degree of interspecific difference of 0.291%–0.3%. The degree of interspecific difference observed between *H. actaeon* and the sequences from *H. bovis* and *H. lineatum* was 12.35% and 12.06%, respectively, similar to that observed by Otranto, Colwell, et al. (2003) and Weigl et al. (2010) and confirming the specific identification of all larvae in our study.

The life cycle of *H. actaeon* is not completely known. We have observed the first-instar larvae covered by a layer of connective tissue without the formation of any subcutaneous nodule or breathing hole and close to the location of second- and third-instar larvae. The finding of a third-instar larva of small size, covered only by connective tissue and fully developed suggests that the life cycle takes place entirely under the skin without intra-organic migrations. Comparable results were obtained by San Miguel et al. (2001) and Panadero et al. (2017), by postmortem examination. However, no other anatomical localizations were examined, and this possibility requires further studies.

In conclusion, this study shows the morphological identification of the three parasitic larval stages of *H. actaeon* (describing the characteristics of the first and second-instar larvae and differentiating them from the third-instar). Moreover, the use of COI allowed the molecular characterization, for the first time, of the first and second-instar larvae of *H. actaeon*.

AUTHOR CONTRIBUTIONS

Sara González: Investigation; methodology; resources; writing – original draft; writing – review and editing. **Maria Luisa Del Rio:** Investigation; methodology; resources; writing – original draft; writing – review and editing. **Maria Natividad Diez:** Investigation; methodology; supervision; writing – review and editing. **Maria del Rosario Hidalgo:** Funding acquisition; investigation; methodology; project administration; resources; supervision; validation; writing – original draft; writing – review and editing. **Angelica Martínez:** Investigation; methodology; supervision; validation; visualization; writing – review and editing.

ACKNOWLEDGMENTS

We are sincerely grateful to the Junta de Castilla y León for providing animals and to all the forestry staff of the "Reserva Regional de Caza de Riaño" by its cooperation. This study was supported by a Research Project 2004-02580-C03-03/BOS from the Spanish "Ministerio de Ciencia y Tecnología" and for the "Grant FIS PI16/00002 (Instituto de Salud Carlos III and cofunded by European Union ERDF/ESF, "Investing in your future")." (English revision by M.C.U. and P.C.U. in acknowledgement).

CONFLICT OF INTEREST

The authors declare no potential conflict of interest.

DATA AVAILABILITY STATEMENT

The data that support the findings of this study are available in GenBank at https://www.ncbi.nlm.nih.gov/genbank/, with the accession numbers: MZ696571, MZ700686, MZ700687, MZ700688, MZ700689, ON540295, ON540296, ON540297, and ON540298.

ORCID

Maria Luisa Del Rio https://orcid.org/0000-0003-3710-2847
Maria Natividad Diez https://orcid.org/0000-0002-1113-9978
Maria del Rosario Hidalgo https://orcid.org/0000-0002-0901-3997
Angelica Martínez https://orcid.org/0000-0001-6631-3817

REFERENCES

Ahmed, H., Ramalho Sousa, S., Simsek, S., Anastácio, S., & Gunyakti Kilind, S. (2017). First molecular characterization of *Hypoderma actaeon* in cattle and red deer (*Cervus elaphus*) in Portugal. *Korean Journal of Parasitology*, *55*, 653–658.

Brauer, F. M. (1863). *Monographie der Oestriden* (p. 291). Druck von Carl Ueberreuter.

Colwell, D. D. (2001). Bot flies and warble flies (Order Diptera: Familiy Oestridae). In W. M. Samuel, M. J. Pybus, & A. A. Kocan (Eds.), *Parasitic diseases of wild mammals* (pp. 60–64). Iowa State University Press.

Colwell, D. D. (2006). Larval morphology. In D. D. Colwell, M. J. R. Hall, & P. J. Scholl (Eds.), *The oestrid flies. Biology, host-parasite relationships, impact and management* (pp. 98–123). CAB International.

Colwell, D. D., Martinez-Moreno, F. J., Martinez-Moreno, A., Hernandez-Rodriguez, S., De la Fuente-Lopez, C., Alunda, J. M., & Hall, M. J. (1998). Comparative scanning electron microscopy of third-instar

Hypoderma spp. (Diptera: Oestridae). *Medical and Veterinary Entomology*, *12*, 181–186.

De la Fuente-López, C., Santín-Durán, M., & Alunda, J. M. (2001). Seasonal changes in prevalence and intensity of *Hypoderma actaeon* in *Cervus elaphus* from Central Spain. *Medical and Veterinary Entomology*, *15*, 204–207.

Domínguez, J., Panadero, R., & De la Fuente-López, C. (2010). Detection of *Hypoderma actaeon* infestation in *Cervus elaphus* with ELISA and western blotting. *Journal of Wildlife Disease*, *46*, 934–938.

Gil-Collado, J., Valls, J. L., & Fierro, Y. (1984). Estudio de los Oestridae y otros artrópodos parásitos de Cervidae de la meseta Sur de España. In *IV Reunión Anual de la Asociación de Parasitólogos Españoles*. Facultad de Farmacia.

Green, M. R., & Sambrook, J. (2012). *Molecular cloning: A laboratory manual* (4th ed.). Cold Spring Harbor Laboratory Press.

Hernández, S., Martínez, F., Calero, R., Moreno, T., & Navarrete, I. (1980). Parásitos del ciervo (*Cervus elaphus*) en Córdoba. I. Primera relación. *Revista Ibérica de Parasitología*, *40*, 93–106.

Martínez-Gómez, F., Hernández, S., Ruiz, R., & Molina, A. (1990). Hypodermosis in the red deer *Cervus elaphus* in Córdoba, Spain. *Medical and Veterinary Entomology*, *4*, 311–314.

Martínez-Moreno, F. J., Navarrete, I., Reina, D., & Hernández-Rodríguez, S. (1997). Deer hypodermosis. *Parassitologia*, *39*, 419–422.

McWilliam, H., Li, W., Uludag, M., Squizzato, S., Park, Y. M., Buso, N., Cowley, A. P., & Lopez, R. (2013). Analysis tool web services from the EMBL-EBI. *Nucleic Acids Research*, *41*, 597–600.

Otranto, D., Colwell, D. D., Traversa, D., & Stevens, J. R. (2003). Species identification of *Hypoderma* affecting domestic and wild ruminants by morphological and molecular characterization. *Medical and Veterinary Entomology*, *17*, 316–325.

Otranto, D., Traversa, D., Guida, B., Tarsitano, E., Fiorente, P., & Stevens, J. R. (2003). Molecular characterization of the mitochondrial cytochrome oxidase I gene of Oestridae species causing obligate myiasis. *Medical and Veterinary Entomology*, *17*, 307–315.

Panadero, R., Martínez-Carrasco, C., León-Vizcaíno, L., López, C., Díez-Baños, P., Morrondo, M. P., & Alonso, F. (2010). Use of a crude extract or purified antigen from first-instar cattle grubs, *Hypoderma lineatum*, for the detection of anti-*Hypoderma* antibodies in free-ranging cervids from southern Spain. *Medical and Veterinary Entomology*, *24*, 418–424.

Panadero, R., Varas, G., Pajares, G., Markina, F., López, C., Díaz, P., Pérez-Creo, A., Prieto, A., Díez-Baños, P., & Morrondo, P. (2017). *Hypoderma actaeon*: An emerging myiasis in roe deer (*Capreolus capreolus*). *Medical and Veterinary Entomology*, *31*, 94–96.

Pérez, J. M., Granados, J. E., & Ruiz-Martínez, I. (1995). Studies on the hypodermosis affecting red deer in central and southern Spain. *Journal of Wildlife Diseases*, *31*, 486–490.

San Miguel, J. M., Álvarez, G., & Luzón, M. (2001). Hypodermosis of red deer in Spain. *Journal of Wildlife Diseases*, *37*, 342–346.

Sugar, L. (1976). On the incidence of larvae of Hypodermatidae in the games and wild rodents of Hungary. *Parasitologia Hungarica*, *9*, 85–96.

Teskey, H. J. (1981). Morphology and terminology-larvae. In J. F. McAlpine, B. V. Peterson, G. E. Shewell, H. J. Teskey, J. R. Vockeroth, & D. M. Wood (Coords.), *Manual of neartic diptera* (Vol. 1, pp. 65–88). Agriculture Canada Research Branch. Monograph 27.

Weigl, S., Traversa, D., Testini, G., Dantas-Torres, F., Parisi, A., Colwell, D. D., & Otranto, D. (2010). Analysis of a mitochondrial noncoding region for the identification of the most diffused *Hypoderma* species (Diptera, Oestridae). *Veterinary Parasitology*, *173*, 317–323.

Wells, J. D., Pape, T., & Sperling, F. A. H. (2001). DNA-based identification and molecular systematics of forensically important Sarcophagidae (Diptera). *Journal of Forensic Sciences*, *46*, 1098–1102.

Wells, J. D., & Sperling, F. A. H. (2001). DNA-based identification of forensically important Chrysomyinae (Diptera: Calliphoridae). *Forensic Science International*, *120*, 110–115.

Zumpt, F. (1965). *Myasis in man and animals in the old world* (pp. 217–229). Butterworths.

How to cite this article: González, S., Del Rio, M. L., Diez, M. N., Hidalgo, M. d. R., & Martínez, A. (2022). Identification of *Hypoderma actaeon* (Diptera: Oestridae) in red deer (*Cervus elaphus*) from northern Spain: Microscopy study and molecular analysis. *Microscopy Research and Technique*, 1–9. https://doi.org/10.1002/jemt.24247